Electron transport and shot noise in double-barrier resonant diodes: The role of Pauli and Coulomb correlations

V. Ya. Aleshkin
Institute for Physics of Microstructures, Nizhny Novgorod GSP-105, 603600, Russia

L. Reggiani
Dipartimento di Ingegneria dell' Innovazione and INFM National Nanotechnology Laboratory, Università di Lecce, Via Arnesano s/n, 73100 Lecce, Italy

(Received 24 February 2001; revised manuscript received 4 June 2001; published 10 December 2001)

We present a theoretical study of electron transport and shot noise in double barrier resonant diodes within the sequential tunneling model. We investigate the role played by Pauli principle and Coulomb interaction on the current voltage (I-V) characteristics and the Fano factor by varying carrier concentration and lattice temperature. At 4.2 K we obtain the bistable I-V characteristics of Z type. In the region of low and intermediate voltages for a sufficiently low electron concentration in the contacts the Fano factor exhibits two successive suppressed regimes associated with Pauli blockade and Coulomb correlation, respectively. By further increasing the voltage shot noise enhancement is found to be a precursor indicator that the device is approaching an instability regime in analogy with the case of phase transitions. In the bistable region hysteresis effects on different transport and parameters are analyzed. At 77 K and increasing temperatures for a carrier concentration of 5×10^{16} cm^{-3} the diode exhibits the usual negative differential conductance (NDC) characteristic. For voltages below NDC only Coulomb correlation remains effective, leading to a suppressed Fano factor intermediate between 0.5–1. For voltages just above NDC a moderate enhancement of the Fano factor up to values around 8 is evidenced. Theoretical findings provide a detailed physical interpretation of experimental results available in the literature and predict features to be confirmed by further experiments.

DOI: 10.1103/PhysRevB.64.245333 PACS number(s): 72.70.+m, 72.20.−i, 73.23.Ad

I. INTRODUCTION

Shot noise is the electrical fluctuation due to the discreteness of the charge which provides direct information on the correlation of different current pulses crossing a device. As such, its determination is of basic complement to a current voltage (I-V) measurement. A convenient analysis of shot noise is usually performed by introducing the dimensionless Fano factor $\gamma \geqslant 0$ defined as $\gamma = S_I(0)/(2qI)$, $S_I(0)$ being the spectral density of current fluctuations at low frequency, I the current flowing in the device, and q the elementary quantum of charge determining I. In the absence of correlation between current pulses it is $\gamma = 1$, and this case corresponds to full shot noise. Deviations from this ideal case is a signature of existing correlations between different pulses and the two possibilities of suppressed (i.e., $\gamma < 1$) and enhanced (i.e., $\gamma > 1$) shot noise are in principle possible.

Shot-noise in double barrier resonant diodes (DBRD's) has received most attention after the first experimental evidence of its suppression by Li and co-workers in 1990.[1] Since then, a series of theoretical analysis of this phenomenon appeared in the literature based on both the coherent[2–7] and the sequential tunneling models.[8–16] From the experimental side, other measurements were performed exploiting both the positive differential conductance (PDC) and the negative differential conductance region (NDC) of the (I-V) characteristics.[10,17–22] Furthermore, experiments became available in a wide range of temperatures from 4.2 to 300 K. The state of the art has been recently reviewed by Blanter and Büttiker.[23]

The salient features of shot noise in DBRD's can be summarized as follows. (i) In the PDC region, suppression is found mainly to a value of 0.5 and in some cases even slightly below down to about 0.2.[10,20] (ii) In the NDC region enhanced is found up to values around 9.[10,21,22] (iii) At increasing temperatures, shot noise suppression is found to smooth out achieving values around 0.6–0.8 at 223–300 K.

The microscopic interpretation of this scenario is based on the correlations occurring between different current pulses crossing the device and associated with the effects of Pauli exclusion principle and Coulomb repulsion. When taken independently, each of these effects would lead normally to shot noise suppression because of the repulsive nature of the correlation. However, in the presence of a strong nonlinearity of the I-V characteristics, the Coulomb repulsion can provide shot noise enhancement through a positive feedback between successive fluctuations of charge number.[5,10,16,17,21,24,25] Even if the main features of shot noise in DBRD are understood, a detailed analysis of the role played by Pauli and Coulomb correlation is still lacking for a quantitative modeling. In particular, the effect of temperature has been only addressed qualitatively.[15]

The aim of this paper is to develop a simple model able to reproduce qualitatively the main features of resonant tunneling in double barrier structures at low bias voltage. The theory is based on a sequential tunneling model and implements that developed by Iannacone *et al.*[15] Accordingly, we are able to explain both sub- and super-Poissonian shot noise behaviors occurring at increasing applied voltages in terms of the interplay between Pauli exclusion principle, Coulomb

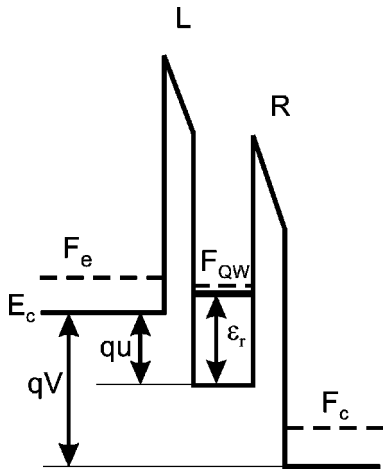

FIG. 1. Sketch of the band profile of the double barrier structure considered here under typical operation conditions.

repulsion and tunneling. The positive feedback between tunneling and space charge, already proposed in the context of a single barrier heterostructure,[24,26–28] is confirmed to be the mechanism responsible for the positive correlation between current pulses. Remarkably, enhanced shot noise is found to act as a precursor indicator that the device is approaching an instability regime characterized by an *I-V* characteristic of *Z* type. For the case of a sufficiently low electron concentration in the contacts, we predict the existence of two consecutive regions of shot noise suppression. In the low-voltage region shot noise suppression is due to the Pauli principle, while in the region just before NDC it is due mainly to Coulomb effects.

The content of the paper is organized as follows. Section II describes the model used. The analytical expressions for the current voltage characteristics and the noise features are presented in Sec. III. The numerical results are discussed for the cases of different carrier concentrations and temperatures in Sec. IV. The major conclusions are drawn in Sec. V.

II. THE MODEL

The structure here investigated is the standard symmetric double well reported in Fig. 1. The essential features of the structure are described by three parameters: the thickness of the two barriers $d_{L,R}=100$ Å, the energy of the resonant level as measured from the center of the potential well $\varepsilon_r=50$ meV, and the partial width of the resonant level due to the tunneling through the left and right barriers $\Gamma=\Gamma_L+\Gamma_R=5$ meV, with $\Gamma_L=\Gamma_R$, which implies an escape time on the 0.1 ps time scale. The chosen values are typical of the symmetric structures used in experiments. We consider the case of sequential tunneling when there is only one resonant state and we assume that the resonant tunneling diode has unit square contacts. Different temperatures are taken in the range $T=4.2$–300 K, and two concentrations of $n=5\times10^{16}$ and 5×10^{17} cm^{-3} in the emitter and collector regions are considered at the lowest temperature.

The kinetic model is developed by assuming that the electron distribution functions in the emitter, in the resonant state, and in the collector are equilibriumlike, but with different electrochemical potentials

$$f(\varepsilon,F_i)=\frac{1}{1+\exp\left(\dfrac{\varepsilon-F_i}{k_BT}\right)}. \tag{1}$$

Here $i=e$ stands for the emitter, $i=$QW for the resonant state, $i=c$ for the collector, k_B is the Boltzmann constant, and ε the carrier energy.

Following Blanter and Büttiker[16] we introduce an effective longitudinal density of states for the resonant states $G_{\rm QW}$, which corresponds to the Breight-Wigner[29] limit for the resonant tunneling:

$$G_{\rm QW}(\varepsilon_z)=\frac{1}{2\pi}\frac{\Gamma}{(\varepsilon_z-\varepsilon_r+qu)^2+\dfrac{\Gamma^2}{4}}, \tag{2}$$

where $-q$ is the electron charge, and u the voltage drop between the emitter and the center of the potential well (see Fig. 1). Equation (2) is a limiting form where the broadening effect associated with the dephasing time is neglected. This point as well as the assumption of constant escape rates have been discussed in Ref. 10 and are outside the scope of the present paper.

The electron flux from the resonant state to the emitter r_1 can be written in the following form:

$$r_1=\frac{m\Gamma_L}{\pi\hbar^3}\int_{E_L}^{\infty}d\varepsilon_z G_{\rm QW}(\varepsilon_z)\int_0^{\infty}d\varepsilon_\perp f(\varepsilon,F_{\rm QW})[1-f(\varepsilon,F_e)], \tag{3}$$

where m is the electron effective mass, $\varepsilon_\perp$ the kinetic energy of the transverse motion, $\varepsilon=\varepsilon_z+\varepsilon_\perp$, and E_L the energy of the bottom of the emitter conduction band. By integrating Eq. (3) over $\varepsilon_\perp$ we find

$$r_1=\frac{2mk_BT\Gamma_L\Gamma}{\pi^2\hbar^3}\times\int_{E_L}^{\infty}\frac{d\varepsilon_z}{[\Gamma^2+4(\varepsilon_z-\varepsilon_r+qu)^2]\left[\exp\left(\dfrac{F_e-F_{\rm QW}}{k_BT}-1\right)\right]}\times\ln\left(\frac{1+\exp\left(\dfrac{F_e-\varepsilon_z}{k_BT}\right)}{1+\exp\left(\dfrac{F_{\rm QW}-\varepsilon_z}{k_BT}\right)}\right). \tag{4}$$

The expression for the electron flux from the resonant state to the collector r_2 can be derived from Eq. (4) by making the substitutions $\Gamma_L\to\Gamma_R$, $F_e\to F_c$, $E_L\to -qu$.

The expressions for the electron flux from the emitter or the collector to the resonant state g_1, g_2, respectively, can be derived from the expressions for r_1 and r_2 by making the substitutions $F_e\leftrightarrow F_{\rm QW}$, $F_c\leftrightarrow F_{\rm QW}$, respectively. We note,

that if the electron concentrations in the emitter and the collector are equal, then $F_c = F_e - qV$, where V is the total applied voltage.

To find the relation between u and V, following Ref. 16 it is supposed that the voltage drops only on the barriers. Accordingly, the charge and voltage drops are connected by the following expressions:

$$u = -Q_e/C_L, \quad V-u = Q_c/C_R. \tag{5}$$

Here $C_{L,R} = \kappa/(4\pi d_{L,R})$ are the capacitances of the left and right barriers, κ the static dielectric constant of the material, and $Q_{e,c}$ the charge of the emitter and collector, respectively.

By using the condition of charge neutrality for the device

$$Q_e + Q_c + Q_{QW} = 0 \tag{6}$$

and Eq. (5) we find

$$V = \frac{u(C_R + C_L) - Q_{\mathrm{QW}}}{C_R}, \tag{7}$$

where $Q_{\mathrm{QW}} = q(N^+_{\mathrm{DQW}} + N_{\mathrm{QW}})$ is the charge in the quantum well, N^+_{DQW}, N_{QW} the concentrations of charged donors and free electrons, respectively, in the quantum well. By using Eqs. (1) and (2) we obtain the expression for N_{QW}:

$$N_{\mathrm{QW}} = \frac{2mk_BT\Gamma}{\pi^2\hbar^2}\int_{E_L-qu}^{\infty} d\varepsilon_z \frac{\ln\left[1+\exp\left(\frac{F_{\mathrm{QW}}-\varepsilon_z}{k_BT}\right)\right]}{\Gamma^2 + 4(\varepsilon_z - \varepsilon_r + qu)^2}. \tag{8}$$

In this model the value of F_e can be calculated from

$$n = N_c F_{1/2}\left(\frac{F_e - E_L}{k_BT}\right). \tag{9}$$

Here n is the electron concentration in the emitter, N_c the effective density of states of the conduction band, and $F_{1/2}(x)$ the Fermi-Dirac integral of index 1/2.[30]

We remark that it is convenient to consider u instead of V as independent variable, since all the values characterizing the device operation are single-valued function of u. Since N_{QW} is only function of u, Eq. (8) can be taken as to define the dependence $V(u)$. Now, from Eq. (3) it follows that both pairs of fluxes $r_{1,2}$, $g_{1,2}$ depend on u and F_{QW}.

The dependence of the electron chemical potential in the resonant state F_{QW} on u is determined by the condition of stationarity, which can be written as

$$g_1 + g_2 = r_1 + r_2. \tag{10}$$

As a general trend, the model so developed is better justified for the following conditions. (i) Voltages should be sufficiently low for the first resonant level to be the only relevant one and for any voltage dependence of the $\Gamma_{L,R}$ resonance width to be negligible. In the present model it implies to consider voltages below about 0.16 V. (ii) Momentum and energy relaxation in the different regions should be sufficiently fast to justify carrier thermalization and as a consequence quasi thermal equilibrium inside the well. This is consistent with the sequential tunneling process where the dephasing time should be shorter than the escape time. Both conditions are well satisfied for applied voltages centered around the current peak controlled by the resonant state, which is the region we are interested in. Therefore, the accuracy of the present model is believed to be adequate for a microscopic interpretation of the salient features of transport and noise in DBRD's as will be discussed below.

III. CURRENT VOLTAGE AND NOISE CHARACTERISTICS

The I-V characteristic is determined by considering I as a parametric function of V. The expression for the current is written

$$I = -q(g_1 - r_1) = -q(r_2 - g_2). \tag{11}$$

To calculate the spectral density of current fluctuations at low frequency S_I we follow the method suggested in Ref. 9 and further developed in Ref. 15. Accordingly, S_I can be expressed by the knowledge of six rates: four being the average electron fluxes defined above for the determination of the I-V characteristics and two being associated with the damping of the fluctuations of N_{QW} through the left ν_1 and right barrier ν_2 respectively,[15] as

$$S_I = 2q^2 \frac{[\nu_2^2(g_1 + r_1) + \nu_1^2(g_2 + r_2)]}{(\nu_1 + \nu_2)^2} \tag{12}$$

and

$$\nu_{1,2} = \nu_{(1,2)r} + \nu_{(1,2)g} \tag{13}$$

with

$$\nu_{(1,2)r} = \frac{dr_{(1,2)}}{dN_{QW}}, \quad \nu_{(1,2)g} = -\frac{dg_{(1,2)}}{dN_{QW}}. \tag{14}$$

The values of the derivatives in Eq. (14) must be taken at $N_{\mathrm{QW}} = \overline{N}_{\mathrm{QW}}$, where the overbar denotes time average. From Eqs. (13) and (14) it is clear that $\nu_{1,2}$ is the change of the total electron flux due to the fluctuation of the number of carriers from the resonant state through the left and right barrier, respectively. These changes govern the dynamics of the fluctuation δN_{QW} as described by the standard Langevin equation in the form

$$\frac{d\,\delta N_{\mathrm{QW}}}{dt} = -\delta N_{\mathrm{QW}}(\nu_1 + \nu_2) + H(t), \tag{15}$$

where $H(t)$ is the stochastic force.

We remark, that if $(\nu_1 + \nu_2) > 0$, then the fluctuation δN_{QW} is damped, which corresponds to a stable condition.

On the contrary, if $(\nu_1+\nu_2)<0$, then the fluctuation $\delta N_{\rm QW}$ is amplified, which corresponds to an unstable condition.

In the following we consider the case of constant total voltage V. To evaluate $\nu_{1,2}$, we note that $g_{1,2}$ and $r_{1,2}$ are functions of the two independent variables u and $F_{\rm QW}$. As a consequence, we need to find the fluctuations δu and $\delta F_{\rm QW}$ which appear due to the fluctuation $\delta N_{\rm QW}$. From Eqs. (7) and (8) we see that under constant voltage it is

$$\delta u = -\frac{q}{C_L+C_R}\delta N_{\rm QW}, \tag{16}$$

$$\delta F_{\rm QW} = -q\,\delta u + \frac{\pi^2\hbar^2\delta N_{\rm QW}}{2mk_BT\Gamma}\left\{\int_0^\infty \frac{dx}{[\Gamma^2+4(xk_BT-\varepsilon_r)^2]\left[1+\exp\left(x-\frac{F_{\rm QW}+qu}{k_BT}\right)\right]}\right\}^{-1}. \tag{17}$$

Thus, it follows that

$$\frac{dg_{1,2}}{dN_{\rm QW}} = -\nu_{(1,2)g} = \frac{\partial g_{1,2}}{\partial u}\frac{\delta u}{\delta N_{\rm QW}} + \frac{\partial g_{1,2}}{\partial F_{\rm QW}}\frac{\delta F_{\rm QW}}{\delta N_{\rm QW}} \tag{18}$$

and

$$\frac{dr_{1,2}}{dN_{\rm QW}} = \nu_{(1,2)r} = \frac{\partial r_{1,2}}{\partial u}\frac{\delta u}{\delta N_{\rm QW}} + \frac{\partial r_{1,2}}{\partial F_{\rm QW}}\frac{\delta F_{\rm QW}}{\delta N_{\rm QW}}. \tag{19}$$

The expressions for $\partial g_{1,2}/\partial u$, $\partial g_{1,2}/\partial F_{\rm QW}$, $\partial r_{1,2}/\partial u$, $\partial r_{1,2}/\partial F_{\rm QW}$ are reported in the Appendix.

The physical meaning of each term entering Eqs. (18) and (19) is the following. The first term on the right-hand side (RHS) of Eq. (18) is connected with Coulomb effects since it describes the change of electron fluxes to the resonant state driven by δu at fixed $F_{\rm QW}$. The δu comes from Coulomb effects as a consequence of the fluctuation $\delta N_{\rm QW}$ and, by moving the resonant level with respect to the occupied electron states in the emitter and the collector, it changes the incoming fluxes. Since $F_{\rm QW}$ is fixed, the occupation of states is fixed and Pauli principle does not contribute to this term. By contrast, the second term on the RHS of Eq. (18) is connected with Pauli principle only. Indeed, this term describes the change in the incoming flux due to the change in the electron occupation of the resonant level when its energy is fixed. In the case of Maxwell-Boltzmann statistics this term equals zero. Analogously, the first term on the RHS of Eq. (19) is of Coulomb nature. The physical origin of the second term on the RHS of Eq. (19) is more complicated than the correspondent of Eq. (18). Indeed, it describes the change in the outcome flux connected with the change in the occupation of the resonant states. There are two contributions to such a change. The first is connected with the rise of the electron number in the resonant states and the second is connected with Pauli principle. In the case of Maxwell-Boltzmann statistics the second contribution is absent and $\partial r_{1,2}/\partial F_{\rm QW} = r_{1,2}/k_BT$.

IV. RESULTS AND DISCUSSION

Here we present the numerical calculations with the main objective of providing a systematic analysis of the electrical and noise properties of DBRD's within the sequential tunneling model. For the material parameters we take those typical of GaAs for the whole structure with $m=0.067\ m_0$ and $\kappa=12.9\ \kappa_0$, m_0 being the free electron mass and κ_0 the vacuum permittivity. To exploit the role played by Pauli and Coulomb correlation, for a given temperature and carrier concentration we report a set of four coupled figures showing

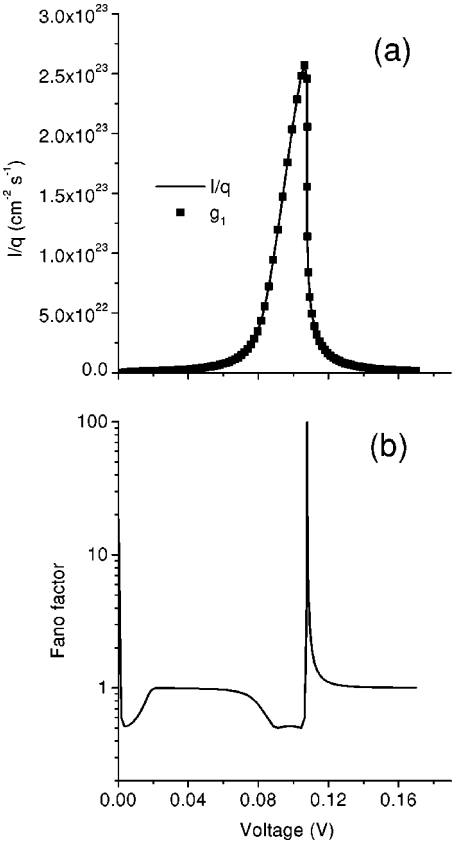

FIG. 2. (a) Current and (b) Fano factor as functions of the applied voltage at $T=4.2$ K and $n=5\times10^{16}$ cm^{-3} for the barrier structure in Fig. 1.

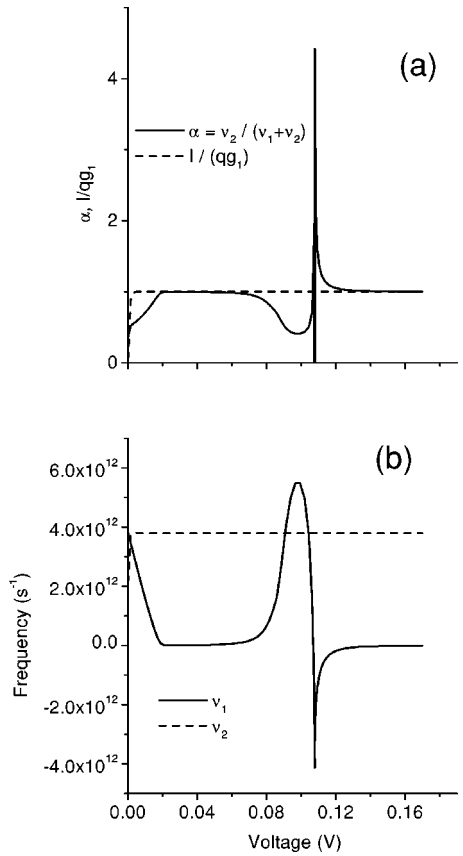

FIG. 3. (a) Normalized rate α and normalized current and (b) ν_1 and ν_2 as functions of the applied voltage at $T=4.2$ K and $n=5\times1^{16}$ cm^{-3} for the barrier structure in Fig. 1.

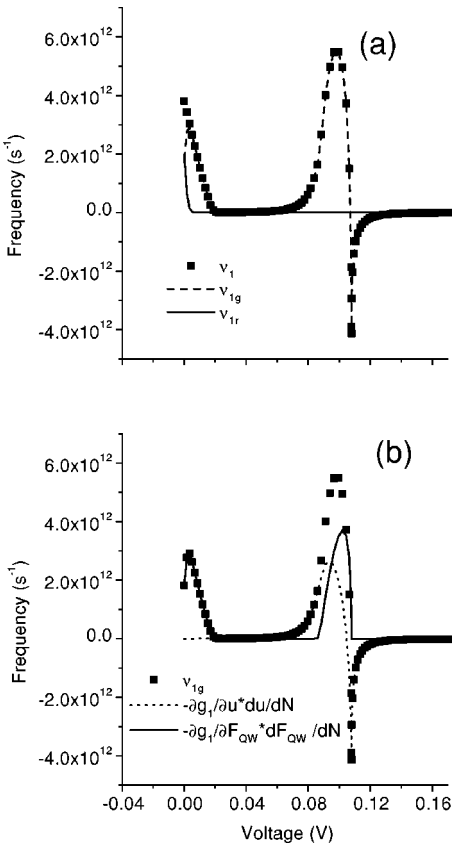

FIG. 4. (a) ν_1 and its contributions ν_{1g}, ν_{1r}; (b) ν_{1g} and its two contributions $\partial g_1/\partial u\times du/dN$, $\partial g_1/\partial F_{\mathrm{QW}}\times dF_{\mathrm{QW}}/dN$ as functions of the applied voltage at $T=4.2$ K and $n=5\times10^{16}$ cm^{-3} for the barrier structure in Fig. 1.

the relevant physical quantities as function of the applied voltage.

A. Low temperature $T=4.2$ K

The case of a low carrier concentration $n_c=5\times10^{16}$ cm^{-3} is reported in Figs. 2 to 5. Figure 2 shows the current [Fig. 2(a)] and the Fano factor [Fig. 2(b)], as function of the applied voltage. After an initial Ohmic region, the current exhibits the typical sharp increase followed by an NDC region controlled by the transmission coefficient of the resonant tunneling. For the values assumed here we found that there is a very narrow region of instability ($V\approx0.11$ V), where there are three current values (branches) corresponding to one value of the voltage (Z-type characteristic). In the unstable branch, originating an intrinsic bistability, we remark that dI/dV is positive. As we shall see later, the Z-type characteristic becomes more pronounced with increasing carrier concentration in the contacts, in agreement with experiments,[31] and it is associated with the feedback between tunneling and space charge. In the whole region of applied voltages the current is found to be determined by the flow of injected particle from the emitter g_1. Concerning the Fano factor, we find that at the lowest voltages ($qV/k_BT<1$) the transition from thermal to shot noise is evidenced. Then, at increasing voltages ($qV/k_BT>1$) we find two separate regions of shot noise suppression matched by a region of full shot noise, and one region of shot noise enhancement. Both suppression minima occur in the PDC region and reach a minimum value $\gamma=0.5$, evidencing the onset of a repulsive correlation between different current pulses. Enhanced shot noise occurs in the bistable region. Strictly speaking, near to the borders of the bistable region the Fano factor goes to infinity, as expected.

To provide a microscopic interpretation of the voltage dependence of the Fano factor, in Figs. 3–5 we present a detailed analysis of the different parameters entering the definition of γ. Figure 3(a) reports the relevant dimensionless parameter $\alpha=\nu_2/(\nu_1+\nu_2)$ and the normalized current $I/(qg_1)$ vs the applied voltage. As it follows from Ref. 28 (see Fig. 3 there), the scenario of the shot noise behavior with $\gamma<1$ when $\alpha<I/(qg_1)$ and with $\gamma>1$ when $\alpha>I/(qg_1)$ is confirmed. Note that almost at all voltages, except when $qV/k_BT<1$, $I/(qg_1)=1$. It means that the back flow from the resonant state to the emitter is absent. This is a consequence of the degeneracy condition (i.e., Pauli blockade) assumed here, which implies that the total current equals the injected one. Figure 3(b) reports the dependencies of $\nu_{1,2}$ on voltage. We can see that ν_1 exhibits a complicate structure at increasing voltages with two positive peaks in the PDC region and one negative peak in the bistable region.

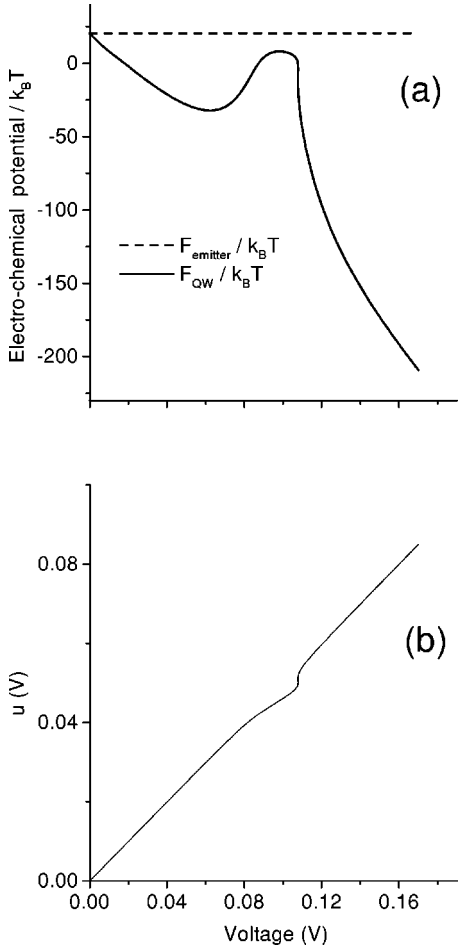

FIG. 5. (a) Electrochemical potentials of the emitter and the quantum well and (b) potential drop between the emitter and the center of the potential well as functions of the applied voltage at $T=4.2$ K and $n=5\times10^{16}$ cm^{-3} for the barrier structure in Fig. 1.

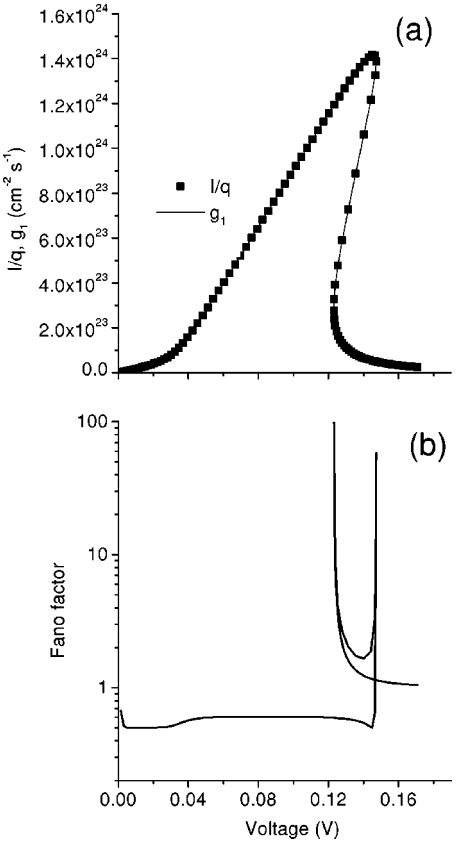

FIG. 6. (a) Current and (b) Fano factor as functions of the applied voltage at $T=4.2$ K and $n=5\times10^{17}$ cm^{-3} for the barrier structure in Fig. 1.

By contrast, ν_2 is constant at almost all voltages. The reason for it is that sooner or later tunneling from the resonant state to the collector will occur. At the smallest voltages, ν_2 decreases due to Pauli principle. At increasing voltages, the condition $\nu_1=\nu_2$ gives $\gamma=0.5$ as expected by the general model of two equal resistors with shot noise sources in series.[32] From Fig. 3(b) we argue that all peculiarities of the Fano factor in essence are controlled by the behavior of ν_1. Thus, in the following we investigate in detail the two contributions in which ν_1 can be decomposed according to Eqs. (13) and (14).

Figure 4(a) reports the dependencies of ν_{1g} and ν_{1r} vs the applied voltage. From the figure we see that, apart from the lowest voltages region, all peculiarities of ν_1 are in essence controlled by ν_{1g}, i.e., they are due to the dependence of the flux of injected electrons upon the number of electrons in the resonant state. Note, that ν_{1r} is small due to the Pauli principle [the same reason leading to $I=(qg_1)$]. In the region of low voltages, when the chemical potential of the resonant state is close to the chemical potential of the emitter, ν_{1r} takes values comparable with ν_{1g}. Figure 4(b) reports the dependencies of the two contributions in which ν_{1g} is decomposed vs the applied voltage. From Figs. 3 and 4 we conclude that at low voltages the first suppression of γ is associated with correlations coming from the Pauli principle (i.e., the term $-\partial g_1/\partial F_{\rm QW}\times dF_{\rm QW}/dN$). The decreasing of this term at increasing voltage is due to the decrease of $F_{\rm QW}$ and hence to the less relevant role played by the Pauli principle at the given temperature. By contrast, the onset in the growth of ν_1 occurring at voltages around 0.8 V, which is responsible for the second suppression of the Fano factor, is mainly due to correlations coming from Coulomb repulsion and associated with $-\partial g_1/\partial u\times du/dN$.

To understand the reason for the rise of $-\partial g_1/\partial u\times du/dN$ here found, we note that when $V<0.11$ V the energy level of the resonant state is higher than that of the bottom of the emitter conduction band E_c. ccordingly, a positive value of δN leads to a negative value of δu and hence to a decrease of g_1. The amount of this decrease is larger when the resonant level is closer to the chemical potential of the emitter, what we can see from Fig. 5(a). The growth of the term $-\partial g_1/\partial u\times du/dN$ is due to the increase of $F_{\rm QW}$ in the region of voltages centered around 0.9 V [see Fig. 5(a)]. We remark that also the instability is due to the Coulomb interaction (as predicted in Ref. 33 and then found in Ref. 31), because $-\partial g_1/\partial u\times du/dN$ is negative in the instability region. The reason for such a negative value is the following. In the instability region the energy level of the

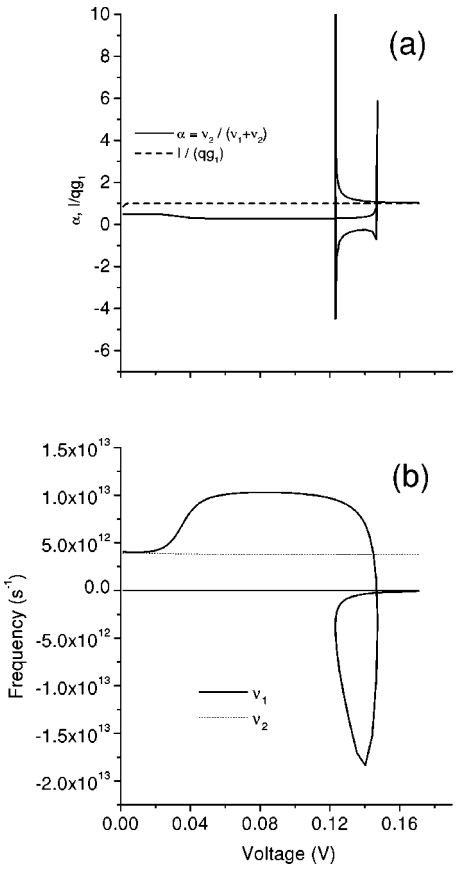

FIG. 7. (a) Normalized rate α and normalized current and (b) ν_1 and ν_2 as functions of the applied voltage at $T=4.2$ K and $n=5\times10^{17}$ cm^{-3} for the barrier structure in Fig. 1.

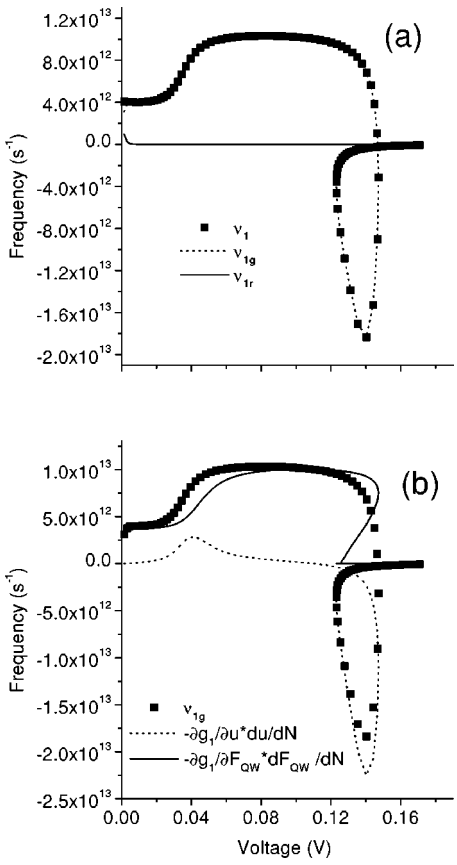

FIG. 8. (a) ν_1 and its contributions ν_{1g}, ν_{1r}; (b) ν_{1g} and its two contributions $\partial g_1/\partial u\times du/dN$, $\partial g_1/\partial F_{\mathrm{QW}}\times dF_{\mathrm{QW}}/dN$ as functions of the applied voltage at $T=4.2$ K and $n=5\times10^{17}$ cm^{-3} for the barrier structure in Fig. 1.

resonance is below E_c. Thus, a negative value of δu, connected with a positive value of δN, increases the electron flux from the emitter to the resonant state, i.e., g_1. This represents a positive feedback for carrier number fluctuations inside the device which is ultimately responsible of the instability. By comparison we remark, that while in the single barrier structure[26,28] the instability was associated with an *S*-type *I*-*V* characteristic and connected with a negative value of ν_2, here it is associated with a *Z*-type *I*-*V* characteristic and due to a negative value of ν_1.

Figure 5(a) reports the dependence of the chemical potential of the resonant state vs applied voltage. The value of the energy difference between the chemical potential and the energy of the conduction band bottom in the emitter is of 7.38 meV. The growth of F_{QW} starting around 0.06 V is due to the high current, since here the energy of the resonant level gets closer to the chemical potential in the emitter. The dependence of the voltage drop between the emitter and the resonant state on voltage is reported for completeness in Fig. 5(b). The presence of space charge is here responsible for the region of nonlinearity exhibited by u at voltages around 0.1 V.

The case of a high carrier concentration of 5×10^{17} cm^{-3} is reported in Figs. 6 to 8. The important differences with the previous case of a lower carrier concentration are associated with the increased importance of degeneracy conditions. In turn, we find an *I*-*V* characteristic with a more pronounced *Z*-type shape [see Fig. 6(a)] and a Fano factor which exhibits hysteresis effects [see Fig. 6(b)]. In particular, in the whole region of PDC, γ remains close to a value of 0.5. In the region of *Z*-type *I*-*V* characteristic γ is always larger than unity, spiking at infinit values in concomitance with the two voltage values related to the onset of the bistable region. From Fig. 7(a) we find again that practically at all voltages the current is determined by g_1 and that γ is determined by α. From Fig. 7(b) we see that again ν_1 is governing the main features of α, even if now it is $\nu_1>\nu_2$ in the suppressed region. From Fig. 8(a) we see that again ν_1 is governed by ν_{1g}, but the region of suppressed shot noise is everywhere controlled by Pauli blockade [see Fig. 8(b)]. From Fig. 8(b) we find that the region of enhanced shot noise is here controlled by the positive feedback between tunneling and space charge. The chemical potential and the voltage drop between the well and the emitter exhibit profiles analogous to those of Figs. 5(a) and 5(b) including nonmonotonic behaviors responsible for hysteresis effects of different transport parameters.

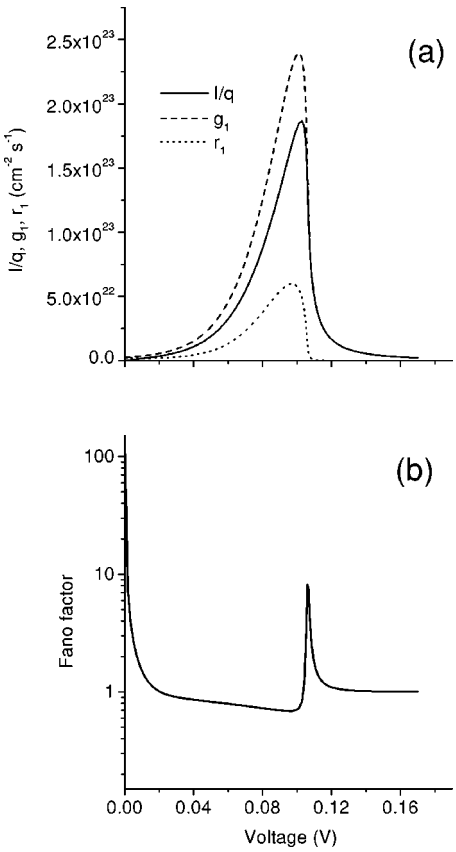

FIG. 9. (a) Current and (b) Fano factor as functions of the applied voltage at $T=77$ K and $n=5\times10^{16}$ cm^{-3} for the barrier structure in Fig. 1.

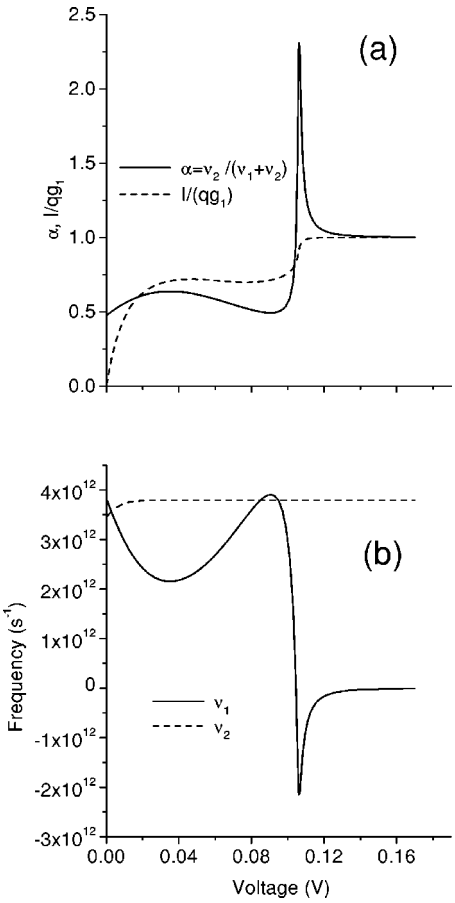

FIG. 10. (a) Normalized rate α and normalized current and (b) ν_1 and ν_2 as functions of the applied voltage at $T=77$ K and $n=5\times10^{16}$ cm^{-3} for the barrier structure in Fig. 1.

B. High temperature $T\geqslant77$ K

The cases of a high temperature of 77 K with a carrier concentration $n_c=5\times10^{16}$ cm^{-3} are reported in Figs. 9 to 11. Here we assist to a vanishing of the effects associated with Pauli exclusion principle, thus only Coulomb correlation is of major significance. The *I-V* characteristics lose the *Z*-type shape in favor of the standard *N*-type NDC, see Fig. 9(a). Furthermore, the contribution of r_1 to the total current becomes of significance. The Fano factor reported in Fig. 9(b) exhibits a suppressed behavior in the PDC region, and an enhanced behavior in the NDC region. Both suppression and enhanced effects are found of decreasing amplitudes with respect to the lower temperature case of 4.2 K seen before. The significant role played by the black flow from the resonant state to the emitter [r_1 contribution in Fig. 9(a)] limits the suppression value to a value of about 0.7. Again, the behavior of the Fano factor at voltages above k_BT/q is essentially controlled by the behavior of α as reported in Fig. 10(a). In particular, enhanced shot noise remains associated with the negativity of ν_1 as, reported in Fig. 10(b). Here, Coulomb correlation is negative (i.e., of repulsion character) in the PDC region, while it provides positive feedback in the NDC region as evidenced by the negative values taken by ν_1 [see Fig. 10(b)].

Figure 11(a) confirms the above interpretation by evidencing the dominant roles played by ν_{1r} and ν_{1g} in the PDC and NDC regions, respectively. Furthermore, the importance of the Coulomb correlation is stressed in Fig. 11(b) which shows the dominant contribution of the term $dg_1/du\times du/dN$ in determining ν_{1g}. For completeness, Fig. 11(c) reports the two contributions in which ν_{1r} is decomposed in analogy with ν_{1g}. It is interesting to note that, even if of minor importance with respect to ν_{1g}, ν_{1r} is dominated by the statistics factor $dr_1/dF_{\mathrm{QW}}\times dF_{\mathrm{QW}}/dN$.

The dependence with applied voltage of the relevant potentials is analogous to that reported in Fig. 5 with behaviors which are more smooth because of the tendency toward nondegenerate conditions. Similar results, which confirm the trend of different transport parameters, have been obtained for $T=300$ K. We have also tested that the essence of the results do not change by changing the value of Γ over two order of magitude. For example, decreasing Γ within a factor of 100 is found to enhance slightly the *Z*-type shape of the *I-V* characteristics at 4.2 K. However, the existence of two separate regions of shot-noise suppression associated with Pauli and Coulomb correlations remains always confirmed.

From the results discussed above we conclude that the agreement found between theoretical calculations and the main features of a large variety of existing experiments validates satisfactorily the model assumed here and the accuracy

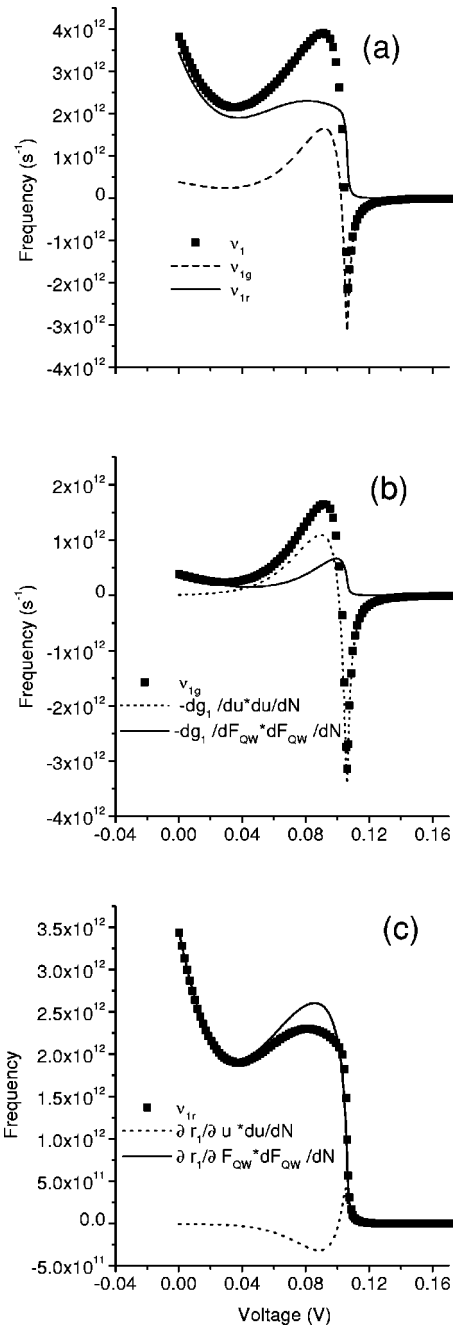

FIG. 11. (a) ν_1 and its contributions ν_{1g}, ν_{1r}; (b) ν_{1g} and its two contributions $\partial g_1/\partial u \times du/dN$, $\partial g_1/\partial F_{\mathrm{QW}} \times dF_{\mathrm{QW}}/dN$; (c) ν_{1r} and its two contributions $\partial r_1/\partial u \times du/dN$, $\partial r_1/\partial F_{\mathrm{QW}} \times dF_{\mathrm{QW}}/dN$ as functions of the applied voltage at $T=77$ K and $n=5\times10^{16}$ cm^{-3} for the barrier structure in Fig. 1.

of the results presented. On this basis, we shed new light in the physical understanding of transport and noise properties in DBRD's operating under the sequential tunneling regime.

V. CONCLUSIONS

Following the approach of Ref. 15 we have developed an analytical theory describing consistently current voltage characteristics and electronic noise associated with current fluctuations in double barrier resonant diodes within the sequential tunneling model. The role of Pauli and Coulomb correlations is investigated as a function of the external applied voltage for different carrier concentrations and temperatures. The comparison between present theoretical findings and available experiments shows the following qualitative main features.

In the PDC region, suppressed shot noise up to Fano factor values around 0.5 is found in agreement with different experiments.[1,10,18,20,21] In particular, the tendency of the suppression to vanish at increasing temperature is well reproduced. The mechanism of suppression can be due to Pauli principle and/or to Coulomb correlation. At the lowest temperature of 4.2 K and for an intermediate carrier concentration below about 5×10^{16} cm^{-3} we predict the possibility to evidence two region of suppressed shot noise separated by a region of full shot noise. At the lowest voltage we find that suppression is due to the predominance of the Pauli mechanism, while before NDC it is the Coulomb mechanism which dominates the suppression. The present model does not explain a suppression below the value $\gamma=0.5$, which was found in some of the experiments[10,20] and theoretically surveyed in Ref. 23.

In the NDC region, enhanced shot noise is in agreement with different experiments.[10,17,21] The mechanism of enhancement is due solely to the positive feedback between tunneling and space charge, and it is a precursor of current instability conditions. These latter should appear in concomitance with a *Z*-type *I*-*V* characteristic, which was observed experimentally by Goldman *et al.*[31]

In summary, we have provided a unified interpretation of the main features exhibited by DBRD's which generally agrees with existing experiments and recovers previous theoretical findings which addressed only partial issues of the subject. In particular, we predict the possibility of observing two sequential shot-noise suppression associated with Pauli and Coulomb correlations before the onset of NDC. Furthermore, under *Z*-type *I*-*V* characteristics interesting features of the Fano factor are its hysteresislike behavior in the region of intrinsic bistability. Some of these predictions look for an experimental confirmation.

ACKNOWLEDGMENTS

Partial support from the Italian Ministry of Foreign Affairs through the Volta Landau Center, the NATO collaborative-linkage Grant No. PST.CLG 976340, and the MADESS II project of the Italian National Research Council (CNR) are gratefully acknowledged.

APPENDIX

In the following we report the explicit expressions of the terms entering Eq. (19) of the main text.

$$\frac{\partial g_1}{\partial u}=-\frac{mqk_BT\Gamma_L\Gamma}{\pi^2\hbar^3}\int_0^\infty d\varepsilon_z\frac{(\varepsilon_z-\varepsilon_r+qu)}{\left(\frac{\Gamma^2}{4}+(\varepsilon_z-\varepsilon_r+qu)^2\right)^2\left[\exp\left(\frac{F_{QW}-F_e}{k_BT}\right)-1\right]}\ln\left[\frac{1+\exp\left(\frac{F_{QW}-\varepsilon_z}{k_BT}\right)}{1+\exp\left(\frac{F_e-\varepsilon_z}{k_BT}\right)}\right], \tag{A1}$$

$$\frac{\partial g_1}{\partial F_{QW}}=\frac{m\Gamma_L\Gamma}{2\pi^2\hbar^3\left[\exp\left(\frac{F_{QW}-F_e}{k_BT}\right)-1\right]}\int_0^\infty d\varepsilon_z\frac{1}{\frac{\Gamma^2}{4}+(\varepsilon_z-\varepsilon_r+qu)^2}\times\left\{\frac{1}{1+\exp\left(\frac{\varepsilon_z-F_{QW}}{k_BT}\right)}-\frac{1}{1-\exp\left(\frac{F_e-F_{QW}}{k_BT}\right)}\ln\left[\frac{1+\exp\left(\frac{F_{QW}-\varepsilon_z}{k_BT}\right)}{1+\exp\left(\frac{F_e-\varepsilon_z}{k_BT}\right)}\right]\right\}, \tag{A2}$$

$$\frac{\partial r_1}{\partial u}=-\frac{mqk_BT\Gamma_L\Gamma}{\pi^2\hbar^3}\int_0^\infty d\varepsilon_z\frac{(\varepsilon_z-\varepsilon_r+qu)}{\left(\frac{\Gamma^2}{4}+(\varepsilon_z-\varepsilon_r+qu)^2\right)^2\left[\exp\left(\frac{F_e-F_{QW}}{k_BT}\right)-1\right]}\ln\left[\frac{1+\exp\left(\frac{F_e-\varepsilon_z}{k_BT}\right)}{1+\exp\left(\frac{F_{QW}-\varepsilon_z}{k_BT}\right)}\right], \tag{A3}$$

$$\frac{\partial r_1}{\partial F_{QW}}=\frac{m\Gamma_L\Gamma}{2\pi^2\hbar^3\left[\exp\left(\frac{F_e-F_{QW}}{k_BT}\right)-1\right]}\int_0^\infty d\varepsilon_z\frac{1}{\frac{\Gamma^2}{4}+(\varepsilon_z-\varepsilon_r+qu)^2}\times\left\{\frac{1}{1+\exp\left(\frac{\varepsilon_z-F_e}{k_BT}\right)}-\frac{1}{1-\exp\left(\frac{F_{QW}-F_e}{k_BT}\right)}\ln\left[\frac{1+\exp\left(\frac{F_e-\varepsilon_z}{k_BT}\right)}{1+\exp\left(\frac{F_{QW}-\varepsilon_z}{k_BT}\right)}\right]\right\}, \tag{A4}$$

$$\frac{\partial g_2}{\partial u}=\frac{m\Gamma_R\Gamma}{\pi^2\hbar^3\left[\exp\left(\frac{F_{QW}-F_c}{k_BT}\right)-1\right]}\int_0^\infty d\varepsilon_z\frac{1}{\frac{\Gamma^2}{4}+(\varepsilon_z-\varepsilon_r)^2}\left\{\frac{1}{1+\exp\left(\frac{\varepsilon_z-qu-F_{QW}}{k_BT}\right)}-\frac{1}{1+\exp\left(\frac{\varepsilon_z-qu-F_c}{k_BT}\right)}\right\}, \tag{A5}$$

$$\frac{\partial g_2}{\partial F_{QW}}=\frac{m\Gamma_R\Gamma}{2\pi^2\hbar^3\left[\exp\left(\frac{F_{QW}-F_c}{k_BT}\right)-1\right]}\int_0^\infty d\varepsilon_z\frac{1}{\frac{\Gamma^2}{4}+(\varepsilon_z-\varepsilon_r)^2}\times\left\{\frac{1}{1+\exp\left(\frac{\varepsilon_z-F_{QW}-qu}{k_BT}\right)}-\frac{1}{1-\exp\left(\frac{F_c-F_{QW}}{k_BT}\right)}\ln\left[\frac{1+\exp\left(\frac{F_{QW}+qu-\varepsilon_z}{k_BT}\right)}{1+\exp\left(\frac{F_c+qu-\varepsilon_z}{k_BT}\right)}\right]\right\}, \tag{A6}$$

$$\frac{\partial r_2}{\partial u}=\frac{m\Gamma_R\Gamma}{2\pi^2\hbar^3\left[\exp\left(\frac{F_c-F_{QW}}{k_BT}\right)-1\right]}\int_0^\infty d\varepsilon_z\frac{1}{\frac{\Gamma^2}{4}+(\varepsilon_z-\varepsilon_r)^2}\left\{\frac{1}{1+\exp\left(\frac{\varepsilon_z-F_c-qu}{k_BT}\right)}-\frac{1}{1+\exp\left(\frac{\varepsilon_z-F_{QW}-qu}{k_BT}\right)}\right\}, \tag{A7}$$

$$\frac{\partial r_2}{\partial F_{QW}} = \frac{m\Gamma_R\Gamma}{2\pi^2\hbar^3\left[\exp\left(\frac{F_c - F_{QW}}{k_BT}\right) - 1\right]} \int_0^\infty d\varepsilon_z \frac{1}{\frac{\Gamma^2}{4} + (\varepsilon_z - \varepsilon_r)^2}$$
$$\times \left\{ \frac{1}{1 - \exp\frac{F_{QW} - F_c}{k_BT}} \ln\left[\frac{1 + \exp\left(\frac{F_c + qu - \varepsilon_z}{k_BT}\right)}{1 + \exp\left(\frac{F_{QW} + qu\varepsilon_z}{k_BT}\right)} \right] \frac{1}{1 + \exp\left(\frac{\varepsilon_z - F_{QW} - qu}{k_BT}\right)} \right\}. \quad \text{(A8)}$$

[1] Y.P. Li, A. Zaslavsky, D.C. Tsui, M. Santos, and M. Shayegan, Phys. Rev. B **41**, 8388 (1990).
[2] L. Chen and C. Ting, Phys. Rev. B **41**, 4534 (1991).
[3] T. Martin and R. Landauer, Phys. Rev. B **45**, 1742 (1992).
[4] S. Hershfield, Phys. Rev. B **46**, 7061 (1992).
[5] M. Jahan and A. Anwar, Solid-State Electron. **38**, 429 (1995).
[6] E. Runge, Phys. Rev. B **47**, 2003 (1993).
[7] H.B. Sun and G. Milburn, Phys. Rev. B **59**, 10 748 (1999).
[8] L. Chen and C. Ting, Phys. Rev. B **46**, 4714 (1992).
[9] J. Davies, P. Hyldgaard, S. Hershfield, and J. Wilkins, Phys. Rev. B **46**, 9620 (1992).
[10] E. Brown, IEEE Trans. Electron Devices **39**, 2686 (1992).
[11] L. Chen, Phys. Rev. B **48**, 4914 (1993).
[12] K. Hung and G. Wu, Phys. Rev. B **48**, 14 687 (1993).
[13] S. Hershfield *et al.*, Phys. Rev. B **47**, 1967 (1993).
[14] J. Egues, S. Hershfield, and J. Wilkins, Phys. Rev. B **49**, 13 517 (1994).
[15] G. Iannaccone, M. Macucci, and B. Pellegrini, Phys. Rev. B **55**, 4539 (1997).
[16] Y.M. Blanter and M. Büttiker, Phys. Rev. B **59**, 10 217 (1999).
[17] T. van de Roer, H. Heyer, and J. Kwaspen, Electron. Lett. **27**, 2158 (1991).
[18] P. Ciambrone *et al.*, Electron. Lett. **31**, 503 (1995).
[19] H.C. Liu, Jianmeng Li, G.C. Aers, C.R. Leavens, M. Buchanan, and Z.R. Wasilewski, Phys. Rev. B **51**, 5116 (1995).
[20] A. Prazadka, K.J. Webb, D.B. Janes, H.C. Liu, and Z.R. Wasilewski, Appl. Phys. Lett. **71**, 530 (1997).
[21] G. Iannaccone, G. Lombardi, M. Macucci, and B. Pellegrini, Phys. Rev. Lett. **80**, 1054 (1998).
[22] V. Kuznetsov, E. Mendez, J. Bruno, and J. Pham, Phys. Rev. B **58**, R10 159 (1998).
[23] Y.M. Blanter and M. Büttiker, Phys. Rep. **336**, 1 (2000).
[24] A. Reklaitis and L. Reggiani, Physica B **272**, 279 (1999).
[25] A. Reklaitis and L. Reggiani, Phys. Rev. B **62**, 16 773 (2000).
[26] V.Y. Aleshkin, L. Reggiani, and A. Reklaitis, Semicond. Sci. Technol. **15**, 1045 (2000).
[27] V.Y. Aleshkin, L. Reggiani, and A. Reklaitis, Nanotechnology **11**, 370 (2000).
[28] V.Y. Aleshkin, L. Reggiani, and A. Reklaitis, Phys. Rev. B **63**, 085302 (2001).
[29] L. Landau and E. Lifshiz, *Quantum Mechanics* (Pergamon Press, Oxford, 1977).
[30] N. Ashcroft and N. Mermin, *Solid State Physics* (Holt, Rinehart and Winston, New York, 1976).
[31] V. Goldman, D. Tsui, and J. Cunningham, Phys. Rev. Lett. **58**, 1256 (1987).
[32] M. Macucci and B. Pellegrini, in *Noise in Physical Systems and 1/f Fluctuations*, edited by P. Handel and A. Chung (AIP, New York, 1993), Vol. 31, p. 284.
[33] B. Ricco and M. Azbel, Phys. Rev. B **29**, 1970 (1984).